MDPI

Article

Lead Isotopes to Identify Underwater Ceramic Contamination: The Example of the Kyrenia Shipwreck (Cyprus)

Virginie Renson * and **Michael D. Glascock**

Archaeometry Laboratory, Research Reactor Center, University of Missouri, 1513 Research Park Drive, Columbia, MO 65211, USA; glascockm@missouri.edu
* Correspondence: rensonv@missouri.edu

Abstract: We present the lead isotopic composition of ceramic fragments from the Kyrenia shipwreck (Cyprus), selected from three chemical groups related to the Rhodes and Alimos regions (Greece). Fragments of the lead sheathing covering the ship's hull and biogenic material formed on some of the ceramic sherds, were analyzed along with sherds from the Rhodes and Alimos source areas for comparison. The objective of this paper was to evaluate the impact of the seawater environment on the isotopic signature of the ceramics, and on our ability to use lead isotopes to source ceramics recovered from seawater. The results showed that the lead isotopic composition of the shipwreck ceramics was modified by its prolonged proximity to the lead hull sheathing. The lead signature of filtering marine organisms encrusted on the ceramics provided support for this hypothesis.

Keywords: lead isotopes; ceramics; shipwreck; seawater; weathering

1. Introduction

Since her discovery in 1967 off the northern coast of Cyprus (Figure 1), the Kyrenia shipwreck and her cargo have been subject of scientific studies focusing on questions related to the hull structure and carpentry techniques, repairs made to the ship over time, material used for her construction, the nature of her cargo, and her journey before she sank off the northern coast of Cyprus, 2200 years ago [1–6]. Over 400 amphorae and other ceramic wares including plates and cooking wares, were recovered during the excavations and subjected to multiple analyses, to identify their provenance and contribute to our understanding of the ship's journey [6].

The elemental chemistry of ceramics from the shipwreck was previously characterized by neutron activation analysis (NAA), with different approaches to data treatment necessary for assigning the ceramics to possible sources [7]. The examination of the NAA results and their comparison with reference groups of ceramics from multiple sources in the Mediterranean suggests at least 11 different provenances for the ceramics found on the shipwreck. In order to achieve this comparison, multiple elements had to be removed, as their concentrations were likely to have been affected by the interaction with seawater. Previous studies of ceramics recovered from underwater have demonstrated that the content in multiple elements can be depleted or enriched [8–12], which makes it difficult to apply this technique for the purpose of provenance, in this particular context.

Lead isotopic analyses have the ability to provide clues on both contamination and provenance of the material from the shipwreck. However, it is well-established that anthropic activities have modified the natural seawater lead isotopic signature and isotopic analyses have long been employed to identify the source of lead present in the marine environment [13–17]. Lead isotopes are also used as a tracer in archaeological science, where they allow tracing of the origin of artifacts by relating them to their geological raw material [18–22]. The recent application of isotopic analysis to archaeological ceramics from multiple contexts in the Eastern Mediterranean and Ancient Mexico, demonstrates that lead isotopes constitute a powerful analytical tool to both discriminate between ceramics of

different origins and to relate ceramics to their source, either by comparison with ceramics of known origin or their raw materials [23,24].
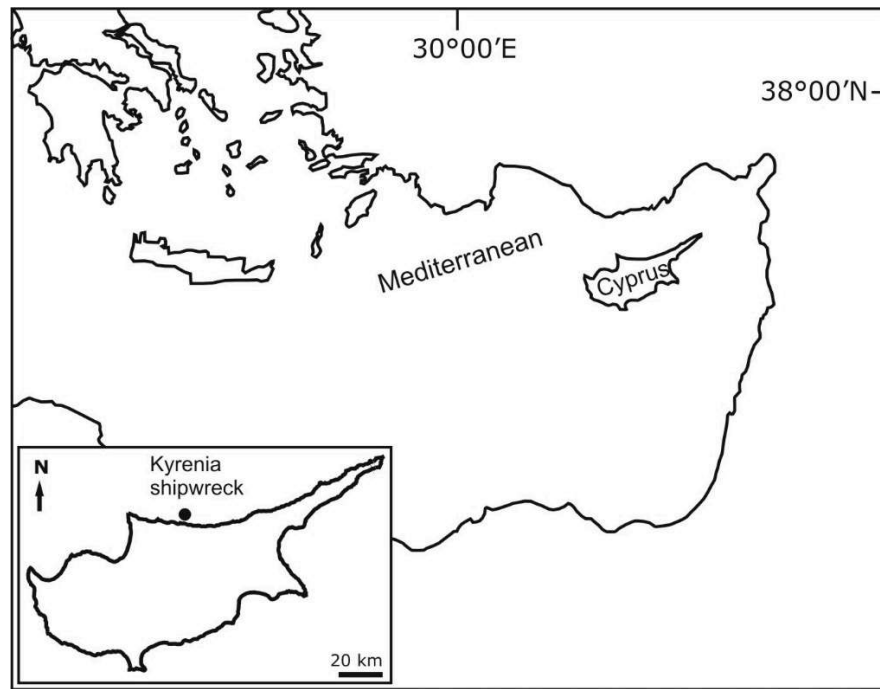

Figure 1. Map and location of the Kyrenia shipwreck.

In this study, we characterize the lead isotopic composition of ceramics recovered from a shipwreck to identify the source of the lead present in these artifacts. Other goals of the study include sourcing the ceramics from the Kyrenia shipwreck in particular, and examining the potential for lead isotopic analysis of ceramics from underwater contexts. For these purposes, lead isotopic analysis was conducted on—(1) ceramics from three different chemical groups assigned to different sources based on NAA, (2) ceramics of known provenance that were used to assign the provenance of some of the ceramics based on NAA, (3) fragments of the lead sheathing that was covering the hull of the ship, and (4) a calcium carbonate encrustation formed by marine organisms that developed on the ceramics.

2. Materials and Methods

2.1. Material

Thirteen ceramic fragments were selected for lead isotope analysis, from among three different chemical groups defined by the recent NAA results [7]. Using an analysis of the Euclidean distance search, the groups investigated here were proposed to be assigned based on elemental chemistry, respectively, to the Rhodes region (group 1, six sherds), to the Alimos, Athens, or Rhodes regions (group 2, five sherds), and to the Attic region (group 3, two sherds).

In addition, as reference groups, six sherds from Alimos and five from Rhodes were analyzed to characterize their lead isotopic composition. The ceramic sherds from Alimos analyzed here correspond to the Late Helladic period and were dated to approximately 1250–1100 BC. They are fragments of closed vessels, dipper, amphora, and stirrup jars that were excavated at Kontopigado. The ceramic sherds from Rhodes correspond to the Hellenistic period and were dated to approximately 400–100 BC. They are fragments of transport amphora and were excavated at Rhodes Town or Villanova. Two fragments of the lead sheathing that was protecting the hull of the ship were also analyzed. The application

of lead sheathing to protect the hull from marine mollusks was common in the Roman period [25] and was employed to protect that of the Kyrenia ship [1]. Finally, one sample of the calcareous deposit formed by marine organisms (skeletons of Bryozoans, tubes of sea worms and conical shell of barnacles) present on some ceramic fragments, was characterized for both lead concentrations and lead isotopes.

2.2. Sample Preparation

2.2.1. Ceramic Assemblage from the Shipwreck and from the Reference Sites

The sherds from the Kyrenia shipwreck were cleaned mechanically using a microdrill equipped with a diamond bit, rinsed with ACS grade methanol and mQ water, and were allowed to dry at room temperature. A rapid surface chemical cleaning was then applied by immersing the fragments in 10 mL of 0.5 M HNO_3 in a PFA Savillex®vial for a brief moment, rinsed with mQ water and immersed in 10 ml of mQ water for deeper rinsing. Samples were dried at room temperature. The sherds from Rhodes and Alimos were cleaned mechanically using a micro drill equipped with a diamond bit, rinsed with PA methanol and mQ water, and were allowed to dry at room temperature. All dried sherds were then ground in an agate mortar. The powders were calcined at 550 °C and finally dried at 105 °C for 24 h. Around 250 mg of powder was digested using 4 mL 24HF, with 1 mL 14N HNO_3 in microwave vessels (190°C for 35 min) and evaporated at 90 °C. The residues were re-digested in 6 ml 6N HCl and transferred to Savillex®vials that were placed on a hot plate at 125 °C for 48 h, and then evaporated at 90 °C.

2.2.2. Marine Calcareous Deposit

Some of the ceramics were covered by a composite calcareous deposit built by marine organisms. Small fragments of the deposit were carefully isolated from one ceramic (sherd P69). The organisms present on that specific sherd were identified as calcareous skeletons of Bryozoans, calcareous tubes of sea worms, and the calcareous conical shell of barnacles [26,27] (Mauro La Russa, pers. com.) (Figure 2). The isolated fragments were examined under a binocular microscope to ensure they were free from minerals/particles from the ceramic. They were then rinsed using mQ water, briefly cleaned using diluted Optima grade HCl, rinsed with mQ water, and dried at 105 °C for 24 h. They were then gently ground in an agate mortar. The deposit was digested in HNO_3, evaporated, re-dissolved in 6N HCl, and evaporated at 90 °C.

2.2.3. Lead Sheathing

Two pieces of the lead sheathing identified as "AIF lead sheathing plotted 5B" and "AHU lead sheathing plotted 6B" were analyzed. A fragment of each piece was isolated using a razor blade and carefully selected from areas that were not too weathered. The two fragments were scraped with the razor blade to mechanically remove as much of the surface deposit as possible. They were then rinsed with mQ water, PA methanol, mQ water, and leached using 5% Optima Grade HCl for 10 min, rinsed five times with mQ water and dried in the oven at 105 °C, for 24 h. Two chips of 15–20 mg were isolated from each fragment using a razor blade. Each chip was transferred in a tube for a deeper chemical cleaning cycle using 6N HCl Optima and with mQ water (2 times), followed by drying in the oven at 105 °C. The four chips were then digested in 2 mL 6N HCl optima at 80 °C for four days, using a graphite warming unit. An aliquot of each solution was taken to obtain approximately 2000 ng of Pb and evaporated in Savillex®vials at 90 °C.
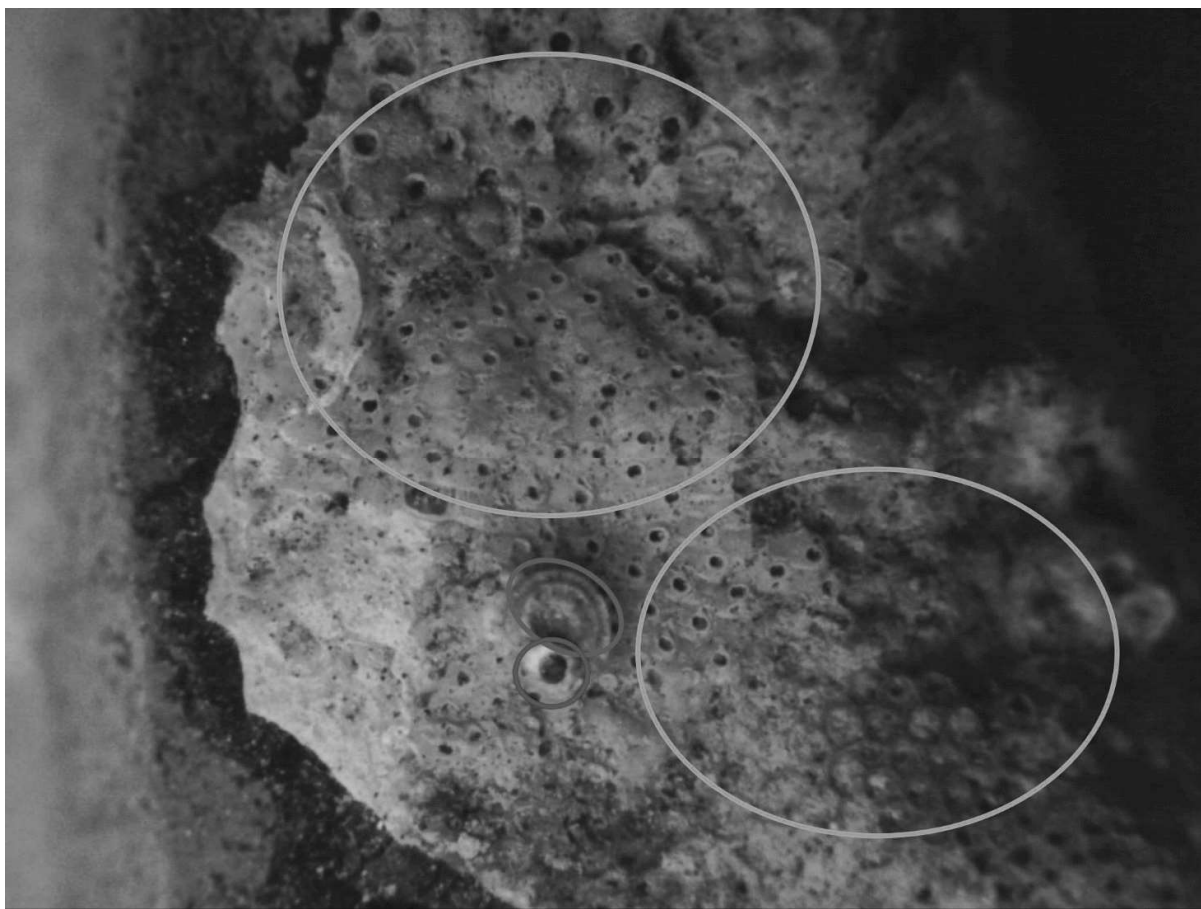
Figure 2. Example of marine organism shells developed on some Kyrenia ceramics. Circled in blue—zones with calcareous skeletons of Bryozoans, circled in red—calcareous tube of sea worm (Polychaetes), and circled in green—conical calcareous shell of Barnacle (Mauro La Russa, pers. com.).

2.3. Lead Isotope Analyses

The dry residues of all samples (ceramics, marine organisms, and lead sheathing) were redigested in 2 mL of HBr and the lead was extracted using AG1-X8 resin loaded on polypropylene columns, using a protocol adapted from Weis et al. [28]. The Pb eluates were evaporated to dryness, the residues were re-digested in 14N HNO_3, evaporated, and re-dissolved in 0.05N HNO_3. Solutions were analyzed on the Nu Plasma II (Nu Instruments) multi collector—inductively coupled plasma—mass spectrometer, in operation at MURR. The SRM981 lead isotopic standard was analyzed multiple times at the beginning of each analytical session, and during analytical sessions after every two samples. Samples and standards were spiked with a Tl solution of the SRM997 and prepared to obtain approximately 250 ng g^{-1} of Pb and 62 ng g^{-1} in Tl. All values obtained for samples and standard were corrected for mass fractionation using the ^{205}Tl/^{203}Tl recommended value 2.38714 (NIST). Measurements were also corrected for isobaric interference of mercury at mass 204. Values obtained for the SRM981 were 36.699 ± 0.009 (2SD), 15.490 ± 0.002 (2SD), and 16.939 ± 0.004, for ^{208}Pb/^{204}Pb, ^{207}Pb/^{204}Pb, and ^{206}Pb/^{204}Pb, respectively. The ratios measured for the samples were finally corrected by standard bracketing [28,29], using the recommended values from Galer and Abouchami [30]. One duplicate (i.e., entire procedure applied twice to the same sample) and four replicates (i.e., repeated measurement of the same solution) were analyzed to evaluate the reproducibility of the method (Table 1).

Table 1. Sample ID; MURR ID; chemical group identified by NAA for the Kyrenia ceramic samples with G1 for the NAA group 1 (assigned to Rhodes), G2 for the NAA group 2 (assigned to Alimos, Athens, or Rhodes), and G3 for the NAA group 3 (assigned to Athens) [7]; lead concentration (µg g^{-1}); lead isotopic ratios; se for standard error (internal error). * for replicates (i.e., second analysis of the same solution on the MC–ICP–MS), ** for duplicates (i.e., entire procedure applied twice to the same sample).

Sample ID	MURR ID	NAA group	[Pb]	1/[Pb]	$^{208}Pb/^{204}Pb$	2se	$^{207}Pb/^{204}Pb$	2se	$^{206}Pb/^{204}Pb$	2se	$^{208}Pb/^{206}Pb$	2se	$^{207}Pb/^{206}Pb$	2se
Alimos 11/22	SHR222				38.8825	0.0015	15.6729	0.0006	18.7362	0.0007	2.07527	0.00003	0.83650	0.00001
Alimos 11/26	SHR226				38.9397	0.0015	15.6835	0.0005	18.7531	0.0007	2.07644	0.00003	0.83631	0.00001
Alimos 11/31	SHR231				38.8898	0.0016	15.6776	0.0007	18.7462	0.0007	2.07455	0.00003	0.83630	0.00001
Alimos 11/36	SHR236				38.8922	0.0016	15.6752	0.0006	18.7532	0.0007	2.07387	0.00003	0.83586	0.00001
Alimos 11/112	SHR312				38.8809	0.0014	15.6733	0.0005	18.7456	0.0006	2.07413	0.00004	0.83611	0.00001
Alimos 11/117	SHR317				38.8845	0.0012	15.6734	0.0005	18.7383	0.0006	2.07515	0.00003	0.83644	0.00001
RHO 08/161	RHO161				38.8939	0.0015	15.6727	0.0005	18.7889	0.0006	2.07007	0.00003	0.83415	0.00001
RHO 08/218	RHO218				38.8892	0.0016	15.6753	0.0006	18.7990	0.0008	2.06868	0.00003	0.83383	0.00001
RHO 08/219	RHO219				38.8782	0.0016	15.6803	0.0006	18.8142	0.0006	2.06646	0.00003	0.83344	0.00001
RHO 08/077	RHO077				38.8370	0.0018	15.6714	0.0007	18.7412	0.0008	2.07228	0.00003	0.83620	0.00001
RHO 08/009	RHO009				38.8978	0.0026	15.6680	0.0006	18.7960	0.0008	2.06948	0.00005	0.83359	0.00002
Kyrenia Type I P38	MUSW144	G1	22.8	0.04	38.9243	0.0020	15.6809	0.0008	18.8712	0.0008	2.06259	0.00004	0.83093	0.00001
Kyrenia Type I P69		G1	15.8	0.06	38.9544	0.0017	15.6828	0.0006	18.8877	0.0007	2.06241	0.00003	0.83032	0.00001
Kyrenia Type I P78	MUSW131	G1	20.2	0.05	38.9257	0.0016	15.6816	0.0006	18.8677	0.0006	2.06307	0.00003	0.83113	0.00001
Kyrenia Type I P114	MUSW104	G1	49.3	0.02	38.8790	0.0015	15.6827	0.0006	18.8565	0.0007	2.06184	0.00003	0.83169	0.00001
Kyrenia Type I P115			13.7	0.07	38.9563	0.0023	15.6793	0.0008	18.8778	0.0006	2.06356	0.00003	0.83056	0.00001
Kyrenia Type I 529	MUSW124	G1	14.6	0.07	38.9466	0.0023	15.6832	0.0009	18.8871	0.0009	2.06210	0.00003	0.83037	0.00002
Kyrenia Type 2 P8	MUSW022	G2	52.0	0.02	38.8841	0.0021	15.6824	0.0009	18.8478	0.0009	2.06302	0.00002	0.83203	0.00001
Kyrenia Type 2 P13	MUSW035	G2	26.1	0.04	38.9239	0.0020	15.6812	0.0007	18.8543	0.0007	2.06444	0.00003	0.83169	0.00001
Kyrenia Type 2 P84	MUSW023	G2	151.8	0.01	38.8753	0.0012	15.6851	0.0005	18.8526	0.0005	2.06208	0.00003	0.83198	0.00002
Kyrenia Type 2 P95	MUSW029	G2	124.1	0.01	38.8683	0.0027	15.6832	0.0007	18.8359	0.0008	2.06350	0.00007	0.83262	0.00003
Kyrenia Type 2 P120	MUSW037	G2	28.6	0.03	38.9034	0.0015	15.6807	0.0006	18.8443	0.0006	2.06444	0.00002	0.83211	0.00001
Kyrenia Type 3 P19/29	MUSW004	G3	112.6	0.01	38.8791	0.0018	15.6845	0.0006	18.8577	0.0007	2.06172	0.00004	0.83173	0.00002
Kyrenia Type 3 P121	MUSW010	G3	26.7	0.04	38.9163	0.0014	15.6792	0.0006	18.7715	0.0007	2.07314	0.00003	0.83527	0.00001
Calcareous Organism			217	0.005	38.8565	0.0015	15.6851	0.0006	18.8526	0.0006	2.06105	0.00003	0.83199	0.00001

Table 1. *Cont.*

Sample ID	MURR ID	NAA group	[Pb]	1/[Pb]	$^{208}Pb/^{204}Pb$	2se	$^{207}Pb/^{204}Pb$	2se	$^{206}Pb/^{204}Pb$	2se	$^{208}Pb/^{206}Pb$	2se	$^{207}Pb/^{206}Pb$	2se
Lead Sheathing 5B Chip 1					38.8600	0.0017	15.6856	0.0006	18.8532	0.0006	2.06123	0.00003	0.83199	0.00001
Lead Sheathing 5B Chip 2					38.8623	0.0023	15.6871	0.0007	18.8562	0.0007	2.06104	0.00007	0.83195	0.00001
Lead Sheathing 6B Chip 1					38.8503	0.0022	15.6838	0.0006	18.8549	0.0010	2.06048	0.00006	0.83182	0.00002
Lead Sheathing 6B Chip 2					38.8725	0.0015	15.6891	0.0006	18.8570	0.0005	2.06150	0.00005	0.83202	0.00001
Alimos 11/22 *					38.8875	0.0019	15.6728	0.0010	18.7365	0.0008	2.07542	0.00003	0.83649	0.00001
Kyrenia Type I P38 *					38.9228	0.0019	15.6803	0.0006	18.8713	0.0007	2.06254	0.00004	0.83091	0.00002
Kyrenia Type 2 P120 *					38.9022	0.0028	15.6791	0.0010	18.8437	0.0010	2.06448	0.00008	0.83206	0.00003
Calcareous Organism *					38.8520	0.0015	15.6845	0.0005	18.8537	0.0005	2.06074	0.00005	0.83191	0.00001
Kyrenia Type I P38 **					38.9265	0.0019	15.6813	0.0007	18.8760	0.0008	2.06220	0.00003	0.83074	0.00001

2.4. Elemental Analysis of the Ceramics

A fraction of the parent solution prepared for isotopic analyses was aliquoted for elemental analysis. The Pb concentrations were measured in the Kyrenia ceramic sherds and the calcium carbonate deposit formed by marine organisms. The Pb concentrations were measured by ICP–MS using a PerkinElmer NexIon 300X operated in KED mode. Solutions were prepared in 3% HNO_3 and internal standards of Sc, In, and Tl were added to the samples. The detection limits were below 0.51 ng Pb.

3. Results

3.1. Kyrenia Samples

Among the ceramic samples from the Kyrenia shipwreck, two groups and a singleton are identified, based on their lead isotopic composition (Figure 3 and Table 1).
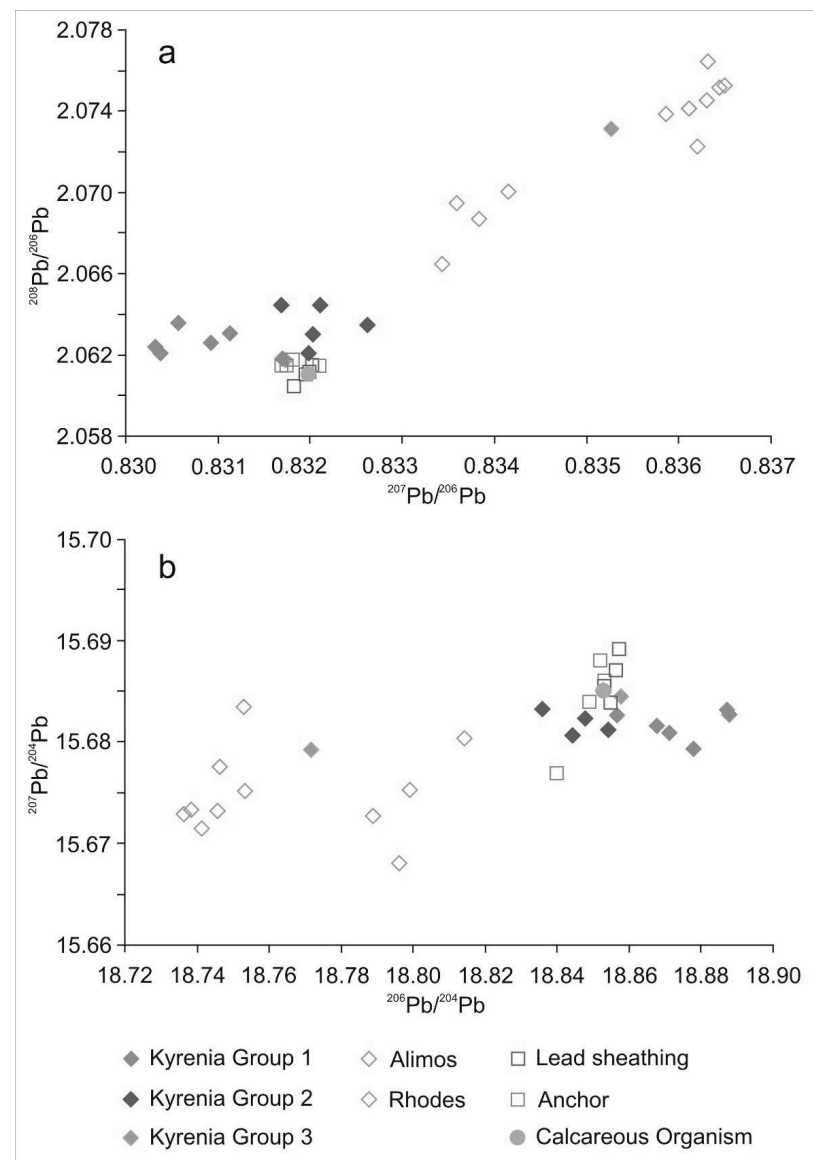
Figure 3. Three-isotope plots for the Kyrenia ceramics presented based on the chemical groups identified by NAA, ceramics from Rhodes and Alimos, the lead from the sheathing, and marine organism shells developed on the Kyrenia ceramics. The values for the anchor are from van Duivenvoorde [5]. (**a**) $^{208}Pb/^{206}Pb$ vs $^{207}Pb/^{206}Pb$, (**b**) $^{207}Pb/^{204}Pb$ vs $^{206}Pb/^{204}Pb$.

One isotopic group is composed of seven samples including five samples of the NAA Group 2, one sample from NAA Group 1, and one sample from NAA Group 3. The lead isotopic composition of this assemblage varies between 15.6807 and 15.6851, between 18.8359 and 18.8577, between 2.06172 and 2.06444, and between 0.83169 and 0.83262, for $^{207}Pb/^{204}Pb$, $^{206}Pb/^{204}Pb$, $^{208}Pb/^{206}Pb$ and $^{207}Pb/^{206}Pb$ ratios, respectively (Figure 3 and Table 1). In the NAA Group 2 fragments, the lead concentration varies between 26.1 ppm and 151.8 ppm, and it is 49.3 ppm in the sample from Group 1 and 112.6 ppm for the sample from Group 3 (Table 1).

A second isotopic group is composed of five samples from the NAA Group 1. The lead isotopic composition of this group varies between 15.6793 and 15.6832, between 18.8677 and 18.8877, between 2.06210 and 2.06356, and between 0.83032 and 0.83113, for $^{207}Pb/^{204}Pb$, $^{206}Pb/^{204}Pb$, $^{208}Pb/^{206}Pb$, and $^{207}Pb/^{206}Pb$ ratios, respectively (Figure 3 and Table 1). The lead concentration in the assemblage varies between 13.7 ppm and 22.8 ppm (Table 1).

The singleton from NAA Group 3 has a lead isotopic composition that presents the values of 15.6792, 18.7715, 2.07314, and 0.83527, for $^{207}Pb/^{204}Pb$, $^{206}Pb/^{204}Pb$, $^{208}Pb/^{206}Pb$, and $^{207}Pb/^{206}Pb$ ratios, respectively (Figure 3 and Table 1), and a lead concentration of 26.7 ppm (Table 1).

3.2. Reference Ceramics from Rhodes and Alimos

The ceramics from Rhodes and Alimos are separated in two groups. One is composed of four samples from Rhodes. The lead isotopic composition of this group varies between 15.6680 and 15.6803, between 18.7889 and 18.8142, between 2.06646 and 2.07007, and between 0.83344 and 0.83415, for $^{207}Pb/^{204}Pb$, $^{206}Pb/^{204}Pb$, $^{208}Pb/^{206}Pb$, and $^{207}Pb/^{206}Pb$ ratios, respectively (Figure 3 and Table 1). The second one is composed of the six samples from Alimos and one sample from Rhodes. The lead isotopic composition of this group varies between 15.6714 and 15.6835, between 18.7362 and 18.7532, between 2.07228 and 2.07644, and between 0.83586 and 0.83650, for $^{207}Pb/^{204}Pb$, $^{206}Pb/^{204}Pb$, $^{208}Pb/^{206}Pb$, and $^{207}Pb/^{206}Pb$ ratios, respectively (Figure 3 and Table 1).

3.3. Lead Sheathing and Calcium Carbonate Deposit

The four lead sheathing samples and the calcareous deposit on the ceramics form a narrow group with a lead isotopic composition that varies between 15.6838 and 15.6891, between 18.8526 and 18.8570, between 2.06048 and 2.06150, and between 0.83182 and 0.83202, for $^{207}Pb/^{204}Pb$, $^{206}Pb/^{204}Pb$, $^{208}Pb/^{206}Pb$, and $^{207}Pb/^{206}Pb$ ratios, respectively (Figure 3 and Table 1). The lead isotopic composition of the lead sheathing also corresponds with that of the lead used in the anchors of the shipwreck [5].

4. Discussion

Groups 1 and 2 have a very similar composition in $^{207}Pb/^{204}Pb$ and $^{208}Pb/^{206}Pb$, but Group 1 has more radiogenic values for $^{206}Pb/^{204}Pb$ and less radiogenic ones for $^{207}Pb/^{206}Pb$ ratio. The range of variation for each group is very small. The two samples from Group 3 present two distinct isotopic compositions.

The recent elemental chemistry results suggest that Group 1 has closest affinities with jars from Rhodes and Group 2 with ceramics from Alimos, Rhodes, or Attica [7]. When compared to the ceramic samples from Rhodes and Alimos analyzed here, none of the samples from Groups 1 and 2 has a lead isotopic composition compatible with the samples from these sources, with both groups from the shipwreck having more radiogenic $^{206}Pb/^{204}Pb$ and less radiogenic $^{208}Pb/^{206}Pb$ and $^{207}Pb/^{206}Pb$ values. Based on elemental chemistry, Group 3 has the closest affinities with Attica. One of the samples from Group 3 has an isotopic signature compatible with that of the material from Alimos. However, the second sample does not have a compatible signature, instead has one that overlaps with samples from Group 2. In terms of provenance, these results do not allow an association with Rhodes over Alimos. The absence of compatibility between Group 1 and the few samples from Rhodes do not, however, exclude the island as a source. At this stage, only

one type of Rhodian jar is used for comparison and likely does not represent the diversity of clays available on the island. The geology of Rhodes is composed of sedimentary rocks, including limestones and flysch (some of which underwent some degree of metamorphism) of different geological age, deposits of lacustrine origins, and the occurrence of ophiolite and diverse quaternary sediments [31], which are likely to provide clays with diverse lead isotopic composition. The samples used here to represent the ceramic production in Rhodes are therefore limited and the analysis of representative clay sources from the island would be necessary to confirm a possible Rhodian origin using lead isotopes. The compatibility between the Rhodes samples and the ceramics from Group 1 are observed, however, based on the elemental chemistry.

The discrepancy between the findings of the elemental analysis and the lead isotopes may be the result of a modification of the isotopic composition of the ceramics. The lead isotopic composition of the samples from Group 2 overlaps with that of the isotopic composition of the lead sheathing, the anchor, and the shells from the marine organisms, but is also compatible with a mixing between the composition of Alimos/Rhodes ceramics and the lead from the sheathing. One sample from Group 1 has a composition similar to that of the sheathing. The other samples from this group, however, do not have a signature that overlaps with that of the sheathing, and their signature is also incompatible with that of a mixing that would result from Alimos/Rhodes as one of the end-members and the lead from the sheathing as the second end-member. For Group 3, the sample that presents the highest lead concentration (sample P19/29, 112.6 μg g^{-1}) has the exact same signature as the lead sheathing, for all ratios. The other sample (sample P121) has a lead isotopic composition that is close to that of the Alimos samples. The lead concentration within a single group is variable (especially in Group 2 and Group 3), which could indicate an enrichment in lead, due to a contamination of the ceramics while underwater. This possibility is further investigated by examining how the isotopic composition varies in relation to the Pb concentration (Figure 4). The plot presenting the isotopic composition vs. 1/[Pb] shows that in Group 1, the ^{208}Pb/^{204}Pb and ^{206}Pb/^{204}Pb values are less radiogenic when the Pb concentration increases but no effect is observed on ^{207}Pb/^{204}Pb (Figure 4). In Group 2, when the Pb concentration increases, the ^{208}Pb/^{204}Pb values are less radiogenic and the ^{207}Pb/^{204}Pb values are more radiogenic, but no effect is observed on the ^{206}Pb/^{204}Pb ratio (Figure 4). In Group 3, the sample presenting high lead concentration (112.6 μg g^{-1}) has a less radiogenic ^{208}Pb/^{204}Pb value and more radiogenic ^{207}Pb/^{204}Pb and ^{206}Pb/^{204}Pb values than the sample presenting lower Pb concentration (26.7 μg g^{-1}) (Figure 4). In all three groups, when an increase in lead content correlates with a variation in the isotopic ratio, the ratios shift towards the lead isotopic composition of the lead from the sheathing, which is also that of the shells of the marine organisms that encrusted the ceramics. The combination of the lead concentrations to that of the lead isotopic ratios observed here is compatible with a contamination of the body of some ceramics by lead from the sheathing.

A recent study conducted on seawater columns surrounding a modern shipwreck showed evidence of contamination of the seawater dissolved and particulate phases, by the metals originating from the ship's hull weathering [32]. In this study, the authors demonstrated that the lead concentrations in the seawater increased from the top to the bottom of the water column, and were also higher downstream from the shipwreck [32]. Similarly, we propose that water in close proximity to the shipwreck may have weathered the lead sheathing, increasing the content of this element in both the dissolved and particulate fraction of the seawater.

Lead in seawater is mainly present in the dissolved fraction where it preferentially bonds with organic ligands. In the inorganic complexes, lead is mainly present as $PbCO_3$ or chlorides [33–35]. Lead present in the dissolved fraction of seawater can be incorporated in the tissues and shells of the filtering marine organisms that act as bio-accumulators. Numerous studies have used mussels as bio-indicators to monitor pollution related to modern human activities [36–42]. Barnacles, or Bryozoans, such as those developed on the ceramics from the shipwreck, also accumulate metals in the bio-mineralizations they produce [43].

The sample of calcium carbonate encrustations formed by marine organisms analyzed here presented a lead concentration of 217 μg g^{-1}. This concentration was abnormally high and above the concentrations reported in the tissues and shells, in modern contexts [36,41,43–46]. This likely results from a lead accumulation by the organisms that developed on the surface of the ceramics, over time, and attests for a contamination of the surrounding seawater by the lead from the sheathing. The presence of bio-colonization and bio-mineralization on underwater artifacts can lead to their alteration [47]. An evaluation of the possible impact of these encrustations on the chemical alteration of the ceramics should also be examined. In the present case, the fragment of encrustation was sampled on a ceramic presenting lower lead concentration, which does not indicate an impact of the encrustations at this point.
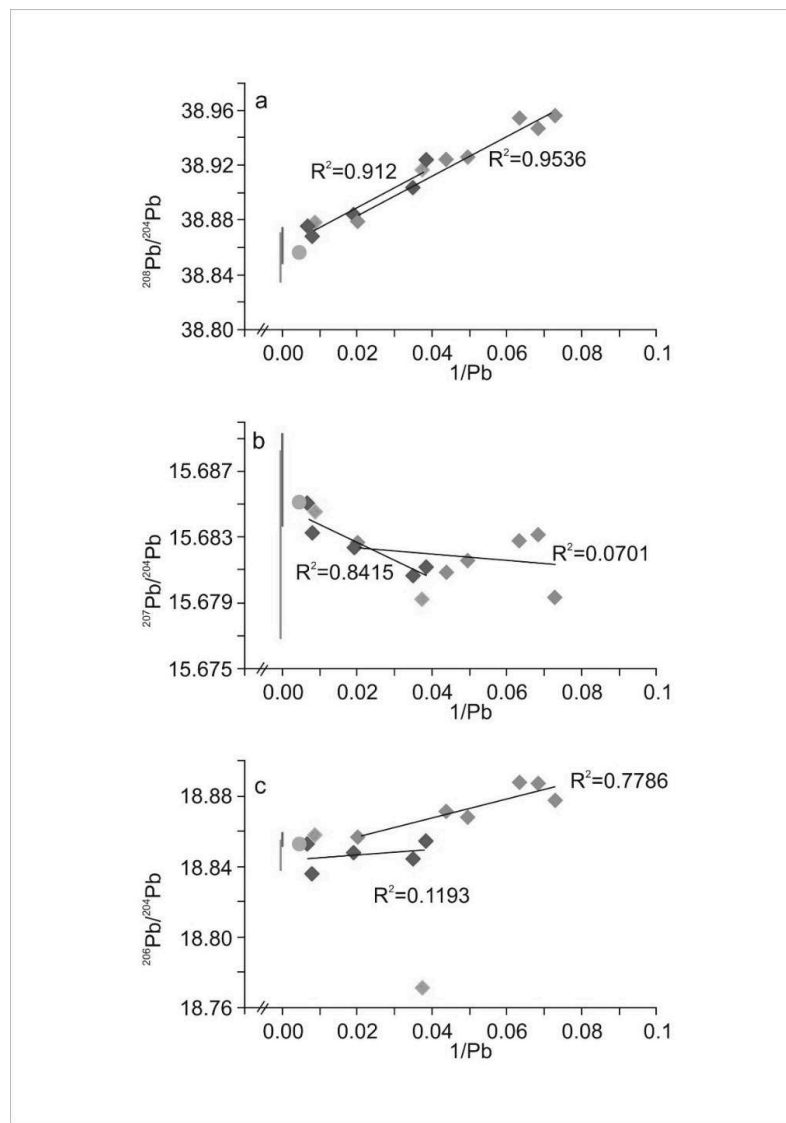

Figure 4. Lead isotopic composition vs. lead concentration. (**a**) ^{208}Pb/^{204}Pb vs. 1/[Pb] (μg g^{-1}), (**b**) ^{207}Pb/^{204}Pb vs 1/[Pb] (μg g^{-1}), and (**c**) ^{206}Pb/^{204}Pb vs 1/[Pb] (μg g^{-1}). Note: The concentrations are reported as 1/[Pb] (μg g^{-1}), so higher concentrations are on the left-side of the x-axis. The red vertical trait symbolizes the lead isotopic composition of the lead sheathing, the light-brown vertical trait symbolizes the lead isotopic composition of the anchor (values reported from van Duivenvoorde [5]). The other symbols are similar to the symbols used in Figure 3.

The results of this first characterization of the lead isotopic signature of underwater ceramics demonstrates the need to consider multiple factors that can affect the original signature of clay-based artifacts in marine contexts. The signature of all potential contributing lead sources, including the duration of the stay underwater, alteration, and biogenic processes, may influence the resulting isotopic composition of the ceramic. This could affect the efficiency of this tool to source clay-based artifacts in this environment and the approach deserves further investigation. This includes characterization of the conditions of burial (presence of sediments to cover the ceramics); development and application of a leaching protocol to eliminate Pb related to post-immersion contamination, as applied to underwater rocks [48]; characterization of the potential clay source or further ceramic types from the potential sources; and examination of the potential impact of biogenic encrustations on the surface of objects, on their chemical composition.

5. Conclusions

This first study of lead isotopic composition of underwater archaeological ceramics from the Kyrenia shipwreck reveals a contamination of the assemblage by lead present in the environment. The evidence supports the lead sheathing that was covering the hull as this source. The proximity of the sheathing to the analyzed materials and their prolonged underwater context (23 centuries) were likely the two main factors that influenced the contamination. This was supported by the lead content and signature of the filtering organisms that accumulated the lead present in the surrounding seawater in their tissues and shells, formed encrustations on the ceramics, and also showed the impact of the lead from the sheathing. At least one ceramic did not show the same signs of alteration.

More broadly, this study demonstrates that the application of lead isotopic analysis to underwater ceramics is promising, pending the characterization of surrounding lead sources and weathering processes that might affect any particular clay-based artifacts.

Further assessment of the usefulness of lead isotope analysis for sourcing ceramics that have been long submerged in seawater is needed. The use of a leaching procedure and the isotopic and elemental characterization of both the leachate and the leached ceramic would be an essential next step. The possible contribution of the development of marine organism shells to the alteration of the chemical signature of clay-based artifacts also deserves examination. In the specific context of the Kyrenia shipwreck, further isotopic characterization of ceramics of known production or raw material would be a useful second phase in this research, as well as a microstructural analysis of the ceramic body of the potsherds. Due to the anthropic impact on the lead cycle and the presence of lead in marine contexts, another critical step in similar contexts would be the characterization of the seawater isotopic composition, either by analyzing the water body in proximity of a shipwreck or that of marine organism encrustations that have developed on the archaeological material or in the vicinity of the material.

Conflicts of Interest: The authors declare no conflict of interest.

References

1. Katzev, M.L. The Kyrenia Shipwreck. *Exped. Mag.* **1969**, *11*, 55–59.
2. Katzev, M.L. The reconstruction of the Kyrenia ship, 1972-1975. *Natl. Geogr. Soc. Res. Rep.* **1981**, *13*, 315–328.
3. Steffy, J.R. The Kyrenia ship: An interim report on its hull construction. *Am. J. Archaeol.* **1985**, *89*, 71–101. [CrossRef]
4. Katzev, S.W. Resurrecting an Ancient Greek Ship: Kyrenia, Cyprus. In *Beneath the Seven Seas*; Bass, G.F., Ed.; Thames and Hudson: New York, NY; London, UK, 2005; pp. 72–79.
5. van Duivenvoorde, W. The anchor of the 3rd-Century-BC ship from Kyrenia, Cyprus: A one-armed wooden anchor with a lead-filled stock. *Int. J. Naut. Archaeol.* **2012**, *41*, 397–407. [CrossRef]
6. Katzev, S.W.; Swiny, L.M. *The Kyrenia Ship Final Excavation Report. Volume I: History of Excavation, Amphoras, Pottery and Coins as Evidence for Dating*; Oxbow Books: Havertown, PA, USA, 2021; p. 464.
7. Glascock, M.D.; Cecil, L.G. Investigating the provenance of ceramics from the Kyrenia ship with neutron activation analysis. In *The Kyrenia Ship Final Excavation Report. Volume II*; Katzev, S.W., Swiny, L.W., Eds.; Oxbow Books: Havertown, PA, USA; p. 464, in press.
8. Bearat, H.; Dufournier, D.; Nouet, Y. Alterations of ceramics due to contact with seawater. *Archaeol. Pol.* **1992**, *30*, 151–162.
9. Pradell, T.; Vendrell-Saz, M.; Krumbein, W.; Picon, M. Altérations de céramiques en milieu marin: Les amphore de l'épave romaine. *Rev. Archéométrie* **1996**, *20*, 47–56. [CrossRef]
10. Montana, G.; Randazzo, L.; Belfiore, C.M.; La Russa, M.F.; Ruffolo, S.A.; De Francesco, A.M.; Pezzino, A.; Punturo, R.; Di Stefano, V. An original experimental approach to study the alteration and/or contamination of archaeological ceramics originated by seawater burial. *Period. Mineral.* **2014**, *83*, 89–120. [CrossRef]
11. Iñañez, J.G.; Bettencourt, J.; Pinto Coelho, I.; Teixeira, A.; Arana, G.; Castro, K.; Sanchez-Garmendia, U. Hit and sunk: Provenance and alterations of ceramics from seventeenth century Angra D shipwreck. *Archaeol. Anthropol. Sci.* **2020**, *12*, 1–16. [CrossRef]
12. Maritan, L. Ceramic abandonment. How to recognise post-depositional transformations. *Archaeol. Anthropol. Sci.* **2020**, *12*, 1–20. [CrossRef]
13. Patterson, C.; Settle, D.; Glover, B. Analysis of lead in polluted coastal seawater. *Mar. Chem.* **1976**, *4*, 305–319. [CrossRef]
14. Patterson, C. Global pollution measured by lead in mid-ocean sediments. *Nature* **1987**, *326*, 244–245. [CrossRef]
15. Véron, A.; Lambert, C.E.; Isley, A.; Linet, P.; Grousset, F. Evidence of recent lead pollution in deep north-east Atlantic sediments. *Nature* **1987**, *326*, 278–281. [CrossRef]
16. Véron, A.; Church, T.M.; Flegal, A.R.; Patterson, C.C.; Erel, Y. Response of lead cycling in the surface Sargasso Sea to changes in tropospheric input. *J. Geophys. Res.* **1993**, *98*, 18269–18276. [CrossRef]
17. Hamelin, B.; Ferrand, J.L.; Alleman, L.; Nicolas, E.; Véron, A. Isotopic evidence of pollutant lead transport from North America to the subtropical North Atlantic gyre. *Geochim. Cosmochim. Acta* **1997**, *61*, 4423–4428. [CrossRef]
18. Farquhar, R.M.; Fletcher, I.R. Lead isotope identification of sources of galena from some Prehistoric Indian sites in Ontario, Canada. *Science* **1980**, *207*, 640–643. [CrossRef] [PubMed]
19. Gale, N.H.; Stos-Gale, Z.A. Bronze Age copper sources in the Mediterranean: A new approach. *Science* **1982**, *216*, 11–19. [CrossRef]
20. Degryse, P. Archeometric applications. In *Isotopic Analysis–Fundamentals and Applications Using ICP-MS*; Vanhaecke, F., Degryse, P., Eds.; Wiley-VCH: Weinheim, Germany, 2012; pp. 373–390.
21. Renson, V.; Jacobs, A.; Coenaerts, J.; Mattielli, N.; Nys, K.; Claeys, P. Using lead isotopes to determine pottery provenance in Cyprus: Clay source Signatures and comparison with Late Bronze Age Cypriote pottery. *Geoarchaeology* **2013**, *28*, 517–530. [CrossRef]
22. Stephens, J.; Killick, D.; Wilmsen, E.; Denbow, J.; Miller, D. Lead isotopes link copper artefacts from northwestern Botswana to the Copperbelt of Katanga Province, Congo. *J. Archaeol. Sci.* **2020**, *117*, 105124. [CrossRef]
23. Renson, V.; Martínez-Cortizas, A.; Mattielli, N.; Coenaerts, J.; Sauvage, C.; De Vleeschouwer, F.; Lorre, C.; Vanhaecke, F.; Bindler, R.; Rautman, M.; et al. Lead isotopic analysis within a multi-proxi approach to trace pottery sources. The example of White Slip II sherds from Late Bronze Age sites in Cyprus and Syria. *Appl. Geochem.* **2013**, *28*, 220–234. [CrossRef]
24. Renson, V.; Neff, H.; Martinez-Cortizas, A.; Blomster, J.P.; Cheetham, D.; Glascock, M.D. Lead and strontium isotopes as tracers for Early Formative pottery exchange in ancient Mexico. *J. Archaeol. Sci.* **2021**, *126*, 105307. [CrossRef]
25. Kahanov, Y.; Ashkenazi, D. Lead sheathing of ship hulls in the Roman period: Archaeometallurgical characterization. *Mater. Charact.* **2011**, *62*, 768–774. [CrossRef]
26. La Russa, M.F.; Ruffolo, S.A.; Ricca, M.; Ricci, S.; Davidde, B.; Barca, D.; Capristo, V. A multidisciplinary approach to the study of underwater artifacts: The case of a *Tritone Barbato* marble statue (Grotta Azzurra, Island of Capri, Naples). *Period. Mineral.* **2013**, *82*, 101–111. [CrossRef]
27. Aloise, P.; Ricca, M.; La Russa, M.F.; Ruffolo, S.A.; Belfiore, C.M.; Padeletti, G.; Crisci, G.M. Diagnostic analysis of stone materials from underwater excavations: The case study of Roman archaeological site of Baia (Naples, Italy). *Appl. Phys. A* **2014**, *114*, 655–662. [CrossRef]
28. Weis, D.; Kieffer, B.; Maerschalk, C.; Barling, J.; de Jong, J.; Williams, G.A.; Hanano, D.; Pretorius, W.; Mattielli, N.; Scoates, J.S.; et al. High-precision isotopic characterization of USGS reference materials by TIMS and MC-ICP-MS. *Geochem. Geophys. Geosystems* **2006**, *7*, Q08006. [CrossRef]

29. White, W.M.; Albarède, F.; Télouk, P. High-precision analysis of Pb isotope ratios by multi-collector ICP-MS. *Chem. Geol.* **2000**, *167*, 257–270. [CrossRef]

30. Galer, S.J.G.; Abouchami, W. Practical applications of lead triple spiking correction of instrumental mass discrimination. *Mineral. Mag.* **1998**, *62A*, 491–492. [CrossRef]

31. Tsombos, P.I.; Nikolakopoulos, K.G.; Photiades, A.; Psonis, K. Updating the 1:50.000 geological maps of Rhodes island using remote sensing data and GIS techniques. In Proceedings of the SPIE 6749, Remote Sensing for Environmental Monitoring, GIS Applications, and Geology VII, 67491H, Florence, Italy, 29 October 2007. [CrossRef]

32. Annibaldi, A.; Illuminati, S.; Truzzi, C.; Scarponi, G. SWASV speciation of Cd, Pb and Cu for the determination of seawater contamination in the area of the Nicole shipwreck (Ancona coast, Central Adriatic Sea). *Mar. Pollut. Bull.* **2011**, *62*, 2813–2821. [CrossRef] [PubMed]

33. Byrne, R.H. Inorganic lead complexation in natural seawater determined by UV spectroscopy. *Nature* **1981**, *290*, 487–489. [CrossRef]

34. Byrne, R.H. Inorganic speciation of dissolved elements in seawater: The influence of pH on concentration ratios. *Geochem. Trans.* **2002**, *3*, 11–16. [CrossRef]

35. Reuer, M.; Weiss, D. Anthropogenic lead dynamics in the terrestrial and marine environment. *Phil. Trans. R. Soc. Lond. A* **2002**, *360*, 2889–2904. [CrossRef]

36. Chow, T.J.; Snyder, H.G.; Snyder, C.B. Mussels (*Mytilus* sp.) as an indicator of lead pollution. *Sci. Total Environ.* **1976**, *6*, 55–63. [CrossRef]

37. Sturesson, U. Lead enrichment in shells of Mytilus edulis. *Ambio* **1976**, *5*, 253–256.

38. Pitts, L.C.; Wallace, G.T. Lead deposition in the shell of the bivalve Mya arenaria: An indicator of dissolved lead in seawater. *Estuar. Coast Shelf Sci.* **1994**, *39*, 93–104. [CrossRef]

39. Boisson, F.; Cotret, O.; Fowler, S.W. Bioaccumulation and retention of lead in the mussel *Mytilus galloprovincialis* following uptake from seawater. *Sci. Total Environ.* **1998**, *222*, 55–61. [CrossRef]

40. Labonne, M.; Ben Othman, D.; Luck, J.-M. Recent and past anthropogenic impact on a Mediterranean lagoon: Lead isotope constraints from mussel shells. *Appl. Geochem.* **1998**, *13*, 885–892. [CrossRef]

41. Shiel, A.E.; Weis, D.; Orians, K.J. Tracing cadmium, zinc and lead sources in bivalves from the coasts of western Canada and the USA using isotopes. *Geochim. Cosmochim. Acta* **2012**, *76*, 175–190. [CrossRef]

42. Steinhardt, J.; Butler, P.G.; Carroll, M.L.; Hartley, J. The application of long lived bivalve sclerochronology in environmental baseline monitoring. *Front. Mar. Sci.* **2016**, *3*, 176. [CrossRef]

43. Amoozadeh, E.; Malek, M.; Rashidinejad, R.; Nabavi, S.; Karbassi, M.; Ghayoumi, R.; Ghorbanzadeh Zafarani, G.; Salehi, H.; Sures, B. Marine organisms as heavy metal bioindicators in the Persian Gulf and the Gulf of Oman. *Environ. Sci. Pollut. Res.* **2014**, *21*, 2386–2395. [CrossRef]

44. Soto-Jiménez, M.F.; Páez-Osuna, F.; Scelfo, G.; Hibdon, S.; Franks, R.; Aggarawl, J.; Flegal, A.R. Lead pollution in subtropical ecosystems on the SE Gulf of California Coast: A study of concentrations and isotopic composition. *Mar. Environ. Res.* **2008**, *66*, 451–458. [CrossRef]

45. Jara-Marini, M.E.; Soto-Jiménez, M.F.; Páez-Osuna, F. Trophic relationships and transference of cadmium, copper, lead and zinc in a subtropical coastal lagoon food web from SE Gulf of California. *Chemosphere* **2009**, *77*, 1366–1373. [CrossRef]

46. El-Sorogy, A.S.; Attiah, A. Assessment of metal contamination in coastal sediments, seawaters and bivalves of the Mediterranean Sea coast, Egypt. *Mar. Pollut. Bull.* **2015**, *101*, 867–871. [CrossRef] [PubMed]

47. Cámara, B.; Álvarez de Buergo, M.; Bethencourt, M.; Fernández-Montblanc, T.; La Russa, M.F.; Ricca, M.; Fort, R. Biodeterioration of marble in an underwater environment. *Sci. Total Environ.* **2017**, *609*, 109–122. [CrossRef] [PubMed]

48. Hanano, D.; Scoates, J.S.; Weis, D. Alteration mineralogy and the effect of acid-leaching on the Pb-isotope systematics of ocean-island basalts. *Am. Mineral.* **2009**, *94*, 17–26. [CrossRef]